



Kinetic analysis of the weak affinity interaction between tris and lysozyme



Tengfei Kang^{a, b, 1}, Wenxin Hao^{a, b, 1}, Yu Niu^a, Ziren Luo^a, Gang Jin^{a, *}

^a NML, Institution of Mechanics, Chinese Academy of Sciences, 15 Bei-si-huan West Road, Beijing 100190, China

^b University of the Chinese Academy of Sciences, 19 Yu-quan Road, Beijing 100049, China

ARTICLE INFO

Article history:

Received 24 December 2014

Available online 19 January 2015

Keywords:

Kinetic analysis

Weak affinity interaction

TIRIE biosensor

Pseudo-first-order interaction kinetics

Association rate constant

ABSTRACT

The biosensor based on total internal reflection imaging ellipsometry (TIRIE), regarded as an automotive real-time research approach for biomolecular interaction, is introduced to analyze the kinetic process of the weak interaction between tris and lysozyme. The experiment is performed by delivering lysozyme solution diluted to different concentrations to the biosensor substrate interface immobilized with tris. By applying pseudo-first-order interaction kinetics model, we are able to obtain the kinetic parameters from fitting experimental data. The calculated association rate constant and dissociation rate constant of tris and lysozyme interaction are in $10^{-2} \text{ mol}^{-1} \text{ s}^{-1}$ and 10^3 s^{-1} magnitude, respectively. To further improve TIRIE's ability for kinetically characterizing biomolecular interaction, a theoretical method to deduce associate rate constant before experiment is proposed.

© 2015 Elsevier Inc. All rights reserved.

1. Introduction

Biomolecular interactions control all kinds of biological phenomenon [1–3], since every life process is resulted in the physical or chemical changes caused by the interactions between biological and chemical molecules, such as neural signal transduction [4], immunological reaction [5], affection of enzyme to substrate [6], and etc. Kinetic analysis of bimolecular interaction process can help us to obtain kinetic parameters and to reveal the laws of life processes [7], especially the weak affinity interaction which usually presents a transient process. Weak affinity interactions, which play significant roles during physiological process in living organisms [8,9], used to being regarded as non-specific and they have been ignored for a long time. With the development of research techniques in recent years [10–12], study of the weak affinity interaction begins available.

There are many experimental methods, including surface plasmon resonance (SPR), enzyme-linked Immunosorbent assays (ELISA), quartz crystal microbalance (QCM) and TIRIE biosensor, now being applied to observe the bimolecular interaction process [13–16]. Working at the total internal reflection mode, TIRIE which

integrated with the imaging ellipsometry system and micro-fluidic system can monitor the real-time bimolecular interaction process with high sensitivity and throughput [17–19]. In our previous work, TIRIE biosensor is proved that it is competent for the detection of the representative weak affinity interaction between tris and lysozyme [20]. However, the kinetics of tris and lysozyme interaction remains unknown. In this paper, we would like to utilize TIRIE biosensor to explore the kinetics between tris and lysozyme.

To improve TIRIE's ability of obtaining kinetic parameters, the commonly used theoretical models, including Langmuir model [21], diffusion particle model [22] and pseudo-first-order interaction kinetics [23], are needed to fit the experimental data. As all the above models can only be applied after the experimental data being collected, the kinetic parameters obtained by the fittings are depended on the experimental data. The pseudo-first-order interaction kinetics, which is closest to the physical pictures of biomolecular interactions taking place in the micro-fluidic system of TIRIE biosensor, is chosen for the kinetic parameters acquisition.

2. Material and methods

2.1. TIRIE biosensor system

The work principle of TIRIE biosensor has been elaborated in Refs. [17,24] and the schematic diagram of its integrated system is shown in Fig. 1. The TIRIE biosensor consists of an imaging

Abbreviations: TIRIE, total internal reflection imaging ellipsometry.

* Corresponding author. Fax: +86 10 82544138.

E-mail address: gajin@imech.ac.cn (G. Jin).

¹ Tengfei Kang and Wenxin Hao have equal contribution to this work.

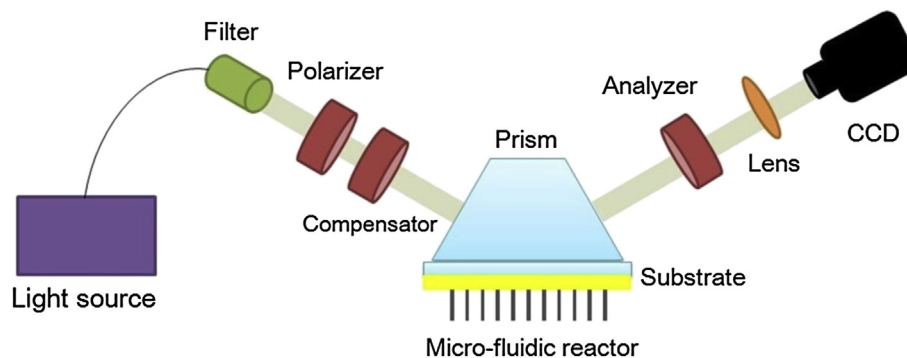


Fig. 1. Schematic illustration of TIRIE biosensor system. Intergrated by an optical detection system and a micro-fluidic reactor system, TIRIE biosensor can real-time monitor the kinetic process of biomolecular interactions.

ellipsometry system which works at the total internal reflection mode and a micro-fluidic reactor system with 24-cells micro-array. A golden substrate, the bottom of which contacts the micro-array reactor and the glass side of which closely link with a prism, is utilized as bio-sensing interface and also optical detection surface. By the substrate, the imaging ellipsometry system can be intergraded with the micro-fluidic reactor system to perform the real-time analysis of bio-molecular interaction process. From the light source, the light beam goes through the polarizer and the compensator and then penetrates into the coupling prism perpendicularly. Since the incident angle set larger than the total internal reflection angle, the light beam is reflected totally at the substrate interface. An evanescent wave appearing at the substrate interface is used to detect the surface mass concentration change induced by the biomolecular interaction on the substrate. By the bio-activity, the ligand molecules immobilized on the substrate interface could capture the target molecules during the flow solution, leading to a change of the surface mass concentration. The micro-fluidic reactor system is made of polydimethylsiloxane (PDMS), which includes a 3×8 cell array and each cell volume is about 150 nL. Any kinds of molecule solution can be individually delivered to each cell by the micro-fluidic system. High-throughput detection can be easily achieved with the combined imaging ellipsometry system with micro-fluidic reactor system. Since the time interval for CCD storage is 0.13 s, the complete process of the biomolecular interaction can be continuously recorded to form a real-time curve (grayscale/time).

2.2. Experimental procedure

TIRIE biosensor substrate is cleaned in piranha solution ($\text{H}_2\text{SO}_4:\text{H}_2\text{O}_2 = 3:1$, v/v) for 30 min and then washed with de-ionized water and pure ethanol alternately for three times. After being dried under pure nitrogen flow, the substrate is immersed into 11-mercaptoundecanoic acid (MUA) ethanolic solution (1 mM) for 18 h. Finally, the modified substrate is rinsed by ethanol and water alternately to remove the excessive MUA.

After the optical settings optimization (the incident angle, the azimuth angle of the polarizer and the analyzer are set to 54° , 163.5° and 131.5° , respectively), the MUA modified substrate is equipped into the TIRIE biosensor system. The first step, 30 μL of a mixture solution prepared with 1-(3-Dimethylaminopropyl)-3-ethylcarbodiimidehydrochloride (EDC) and N-hydroxyl-succinimide (NHS) at the concentration of 0.2 mol/ml and 0.05 mol/ml in deionized water is passed across the interface of the substrate at a flow rate of 5 $\mu\text{L}/\text{min}$, by the micro-fluidic system. After rinsing with phosphate buffered saline (PBS), 75 μL of 1 M tris is delivered

to each reaction cell at a flow rate of 5 $\mu\text{L}/\text{min}$ to immobilize tris on the sensing surface. And then, PBS is added to each reaction cell to rinse the tris surface. After that, 25 μL of lysozyme solutions whose concentration ranges from 6.6 μM to 33 μM is delivered to the tris-immobilized surface at a flow rate of 5 $\mu\text{L}/\text{min}$. Eventually, PBS is passed to all the reaction cells to rinse the substrate.

3. Results

3.1. Kinetic analysis with the first order reaction kinetic model

TIRIE biosensor provides us with a method to analyze the kinetics of the weak affinity interaction between tris and lysozyme, and the real-time curves recorded by TIRIE biosensor for tris and lysozyme interaction are presented in Fig. 2. Due to the weak binding between the two molecules¹⁴, the real-time curves appear a typical transient reaction trend that the complex formed by the two molecules dissociates after PBS injection. To resolve the kinetic parameter of the interaction between tris and lysozyme, the pseudo-first-order interaction kinetics which relates to the one-step simple reactions is introduced (see Eq. (1)) [25].

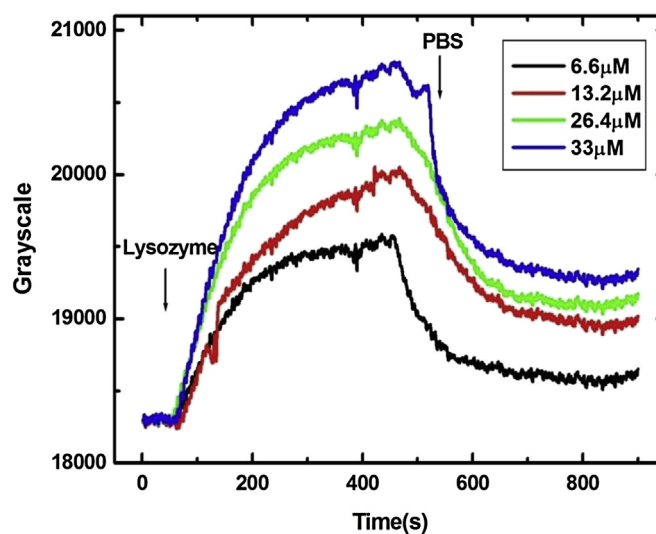


Fig. 2. The real-time curve for the interaction between tris and lysozyme at different concentrations. During 60s, lysozyme at the concentrations of 6.6, 13.2, 26.4 and 33 μM is delivered to the tris immobilized surface, which increases the sensor signal. When PBS injected for rinsing the surface, the sensor signal decrease, indicating that the complex formed by tris and lysozyme is unstable.

$$\frac{dc_{AB}}{dt} = k_{on}c_Ac_B - k_{off}c_{AB} \quad (1)$$

where dc_{AB}/dt is the net rate to form the complex of tris and LZM. k_{on} and k_{off} are the association and disassociation rate constants, respectively. c_{AB} indicates the amount of compound AB, c_A and c_B represent the concentration of the ligand and target molecule. According to the description in Refs. [26], the ordinate of the experimental results can be converted from grayscale to surface density by Eq. (2),

$$s = 0.113 \times \left(\frac{I - I_0}{K} \right) \quad (2)$$

During the formation, s and I represent the surface density and the grayscale value respectively. The number in formulation is determined by the initial grayscale in the experiments and the Lorentz–Lorenz theory [27]. After the ordinate of the experimental data converted from grayscale to surface density, the real-time curves of the two molecules binding part are fitted using pseudo-first-order interaction kinetics model. The fitting plots and kinetic results are shown in Fig. 3 and Table 1, respectively.

As shown in Table 1, with the dissociation constant (K_D) calculated to 10^{-5} M magnitude, tris and lysozyme interaction belong to the weak affinity interactions, which is defined as K_D more than 10^{-6} M. And the association rate constant (k_{on}) acquired is in 10^2 M s $^{-1}$ magnitude; while k_{on} in the strong affinity interactions is generally more than 10^3 M s $^{-1}$. It is induced by the reason that tris molecule reacts lysozyme molecule with hydrogen bond [28], in which the bond energy is only equivalent to 1/10 of that in covalent binding.

3.2. k_{on} acquisition by a theoretical method

For further verifying the accuracy of kinetic parameters obtained by the pseudo-first-order interaction kinetics model, a theoretical approach to deduce k_{on} is proposed. Compared with the traditional posterior-type models, the theoretical method could predict k_{on} before experiment. The establishment of the theoretical method is based on the assumption of pseudo-first-order interaction. Several experimental conditions, such as temperature, flow quantity, binding energy and coverage rate of binding site, have been considered in the theoretical approach to deduce k_{on} quantitatively. The expression of k_{on} is shown as

$$k_{on} = a \cdot Q \cdot N_0 \cdot \frac{1}{1 + e^{-\Delta E/kT}} \quad (3)$$

where a is the cross sectional area of ligand molecule, T means temperature and ΔE is the binding energy. Q represents the flow quantity of target molecule and N_0 is Avogadro's constant. The detailed derivation of k_{on} is eliminated in Appendix A. The above equation indicates that k_{on} is independent of the target molecule concentration and the surface density of the ligand molecule immobilized on the sensing surface, so all the related parameters could be obtained from the reference or the experimental conditions before the experiment.

According to Eq. (3) and the data shown in Table 2, k_{on} is calculated to 2.26×10^2 mol $^{-1}$ s $^{-1}$, which is in good agreement with the result by fitting experimental data (the deviation between experimental results and theoretical results is less than 5%). This result confirms the accuracy of k_{on} obtained by the pseudo-first-

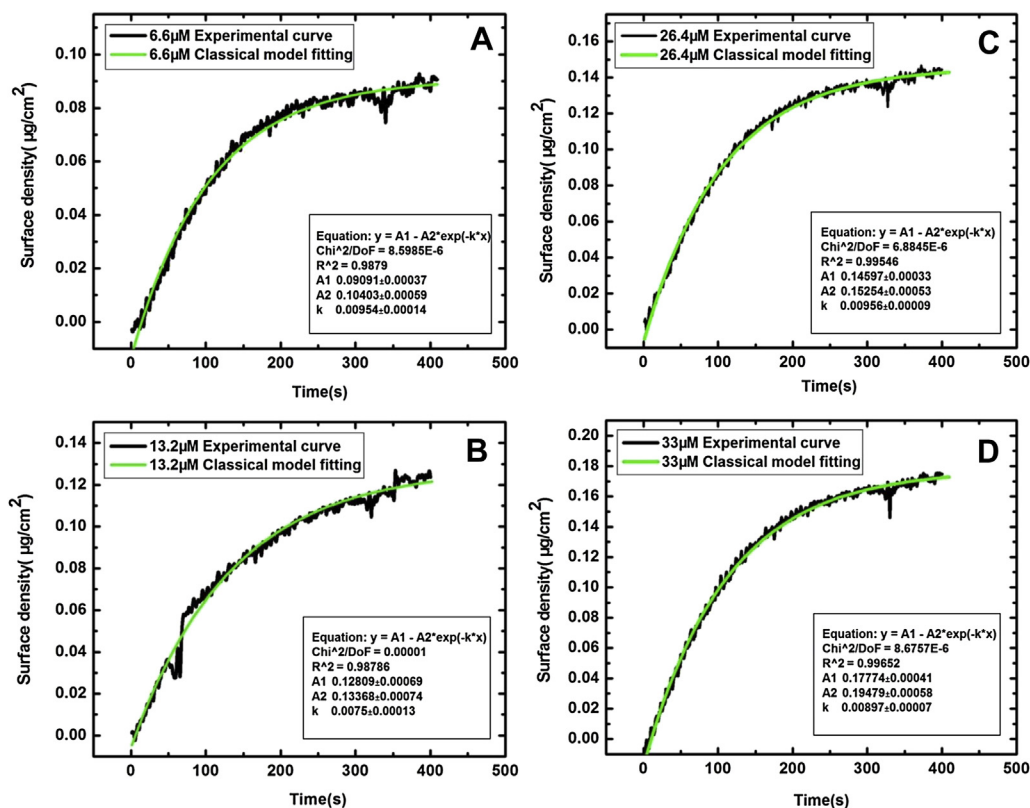


Fig. 3. Curve-fitting of the surface density curve for lysozyme at different concentrations. The black curve represents the experimental results. The green curve expresses the simulation curve of the first order reaction kinetic model. (A) (B) (C) (D) represent the curve for lysozyme at 6.6, 13.2, 26.4 and 33 µM, respectively. (For interpretation of the references to color in this figure legend, the reader is referred to the web version of this article.)

Table 1
Kinetic parameters of lysozyme at different concentrations binding to tris immobilized on the sensing surface. Experimental data is fitted to the first order reaction kinetic model.

Ligand	Target	Concentration	k_{on} ($\text{mol}^{-1} \text{s}^{-1}$)	k_{off} (s^{-1})	K_D (M)
Tris	Lysozyme	6.6 μM	$1.9 \pm 0.2 \times 10^2$	$3.3 \pm 0.5 \times 10^{-3}$	$1.74 \pm 0.15 \times 10^{-5}$
		13.2 μM	$2.4 \pm 0.4 \times 10^2$	$4.6 \pm 0.9 \times 10^{-3}$	$1.92 \pm 0.37 \times 10^{-5}$
		26.4 μM	$2.1 \pm 0.1 \times 10^2$	$3.8 \pm 0.4 \times 10^{-3}$	$1.81 \pm 0.28 \times 10^{-5}$
		33 μM	$2.2 \pm 0.3 \times 10^2$	$3.1 \pm 0.6 \times 10^{-3}$	$1.41 \pm 0.41 \times 10^{-5}$

order interaction kinetics model and also indicates that the theoretical method is competent for deducing k_{on} .

4. Discussion

TIRIE biosensor has been introduced to analyze the kinetics of the weak affinity interaction between tris and lysozyme. The kinetic process of tris and lysozyme interaction is real-time recorded by TIRIE biosensor. With the traditional posterior-type model, kinetic parameters are acquired by fitting the experimental data. For confirming the accuracy of fitting results, a theoretical method, based on the assumption of the pseudo-first-order interaction and the physical picture of biomolecular interaction occurring in TIRIE biosensor, has been proposed to deduce k_{on} of tris and lysozyme interaction before experiment. The theoretical results are in good agreement with the experimental results. These results imply that TIRIE biosensor is an effective tool for the kinetic examine of weak affinity interactions.

This is the first time reported that kinetic parameters are deduced by a theoretical method, rather than simulation methods or fitting experimental results. For the traditional posterior-type model, the theoretical method regarded as a priori-method is an excellent supplement and development. By introducing the priori-method, the instability of kinetic parameter calculated by posterior-type model, which induced by the experiment conditions, can be effectively reduced.

Conflict of interest

The authors have no conflict of interest.

Acknowledgments

The authors acknowledge the financial support to the National Basic Research Program of China (2015CB352100), to the National Natural Science Foundation of China (21305147, 81472941), to the International Science & Technology Cooperation Program of China (2012DFG31880), and to the Seventh Sino-Portugal Scientific and Technological Cooperation of 2013–2015.

Appendix A. k_{on} theoretical derivation

To predict k_{on} before carrying out experiment, a theoretical method has been established on the first order reaction kinetic model and the experimental condition of the micro-fluidic reactor in TIRIE biosensor as shown in Fig. 4.

A typical biomolecular interaction can be expressed by Eq. 4. A and B represent the target molecule and the ligand molecule,

Table 2
Related data for k_{on} expression (a, b from protein data bank).

Interaction	Cross sectional area (a)	Temperature (T)	Flow quantity(Q)	Binding energy (ΔE)
Tris-lysozyme	$5 \times 10^{-19} \text{m}^2$ ^a	293 K	5 $\mu\text{L}/\text{min}$	$3.51 \times 10^{-20} \text{J mol}^{-1}$ ^b

respectively, while AB is the compound formed due to the bio-activity between A and B.



By utilizing a peristaltic pump, a steady and continuous liquid flow of molecule A solution can be delivered to the substrate and react with B. During the interaction, the concentration of molecule A can be regarded as a constant due to the continuous delivery of its solution. Within a unit time, the amount of molecule A that arrives at the sensor surface can be expressed as:

$$N_A = c_A \cdot Q \cdot N_0 \quad (5)$$

where c_A represents the concentration of molecule A, Q means flow quantity and N_0 is Avogadro's constant. Within N_A , only a fraction of molecule A can encounter molecule B, since molecule B may not cover the entire sensor surface. The coverage rate of molecule B on the interaction surface may be given as:

$$R_B = a \cdot s_B \quad (6)$$

where a is the cross sectional area of molecule B and s_B represents the surface density of molecule B immobilized on the sensor surface. The information of a can be obtained in Protein data bank. When molecule A contacts with molecule B, the probability that they can chemically combine obeys Boltzmann's law [29], as follows:

$$P_{AB} = \frac{1}{1 + e^{-\Delta E/kT}} \quad (7)$$

ΔE is the binding energy which has been acquired. Therefore, the increase of the surface density of AB due to the interaction between A and B per unit time can be given as:

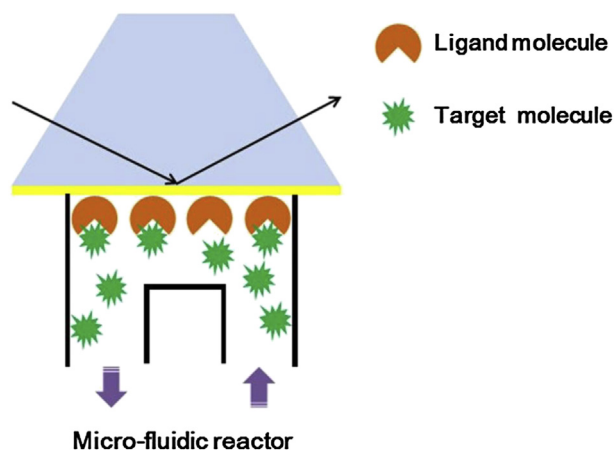


Fig. 4. The physical picture of the interaction between ligand molecule and target molecule in the micro-fluidic reactor of TIRIE system.

$$\Delta S_{AB} = N_A \cdot R_B \cdot P_{AB} = c_A \cdot Q \cdot N_0 \cdot a \cdot s_B \cdot \frac{1}{1 + e^{-\Delta E/kT}} \quad (8)$$

The increase of the surface density of AB per unit time in the pseudo-first-order interaction kinetics is expressed as:

$$\Delta S_{AB} = k_{on} \cdot c_A \cdot s_B \quad (9)$$

Thus, compared with Eq. (9), we have

$$k_{on} = a \cdot Q \cdot N_0 \cdot \frac{1}{1 + e^{-\Delta E/kT}} \quad (10)$$

The above equation indicates that k_{on} is independent of c_A and s_B and all the parameters can be obtained from the reference or the experimental conditions before experiment.

Transparency document

The transparency document associated with this article can be found in the online version at <http://dx.doi.org/10.1016/j.bbrc.2015.01.044>.

References

- [1] A.E. Nel, L. Madler, D. Velegol, T. Xia, E.M. Hoek, P. Somasundaran, F. Klaessig, V. Castranova, M. Thompson, Understanding biophysicochemical interactions at the nano-bio interface, *Nat. Mater.* 8 (2009) 543–557.
- [2] J.F. Stevens, C.S. Maier, Acrolein: sources, metabolism, and biomolecular interactions relevant to human health and disease, *Mol. Nutr. Food Res.* 52 (2008) 7–25.
- [3] T. Yamada, P. Bork, Evolution of biomolecular networks: lessons from metabolic and protein interactions, *Nat. Rev. Mol. Cell. Biol.* 10 (2009) 791–803.
- [4] G.C. Brainard, M.D. Rollag, J.P. Hanifin, Photic regulation of melatonin in humans: ocular and neural signal transduction, *J. Biol. Rhythms* 12 (1997) 537–546.
- [5] F. Debierre-Grockiego, R.T. Schwarz, Immunological reactions in response to apicomplexan glycosylphosphatidylinositols, *Glycobiology* 20 (2010) 801–811.
- [6] W. Li, D. Tu, A.T. Brunger, Y. Ye, A ubiquitin ligase transfers preformed poly-ubiquitin chains from a conjugating enzyme to a substrate, *Nature* 446 (2007) 333–337.
- [7] M.J. Cannon, A.D. Williams, R. Wetzel, D.G. Myszk, Kinetic analysis of beta-amyloid fibril elongation, *Anal. Biochem.* 328 (2004) 67–75.
- [8] I.M.A. Nooren, J.M. Thornton, Structural characterisation and functional significance of transient protein–protein interactions, *J. Mol. Biol.* 325 (2003) 991–1018.
- [9] M.L. Dustin, D.E. Golan, D.M. Zhu, J.M. Miller, W. Meier, E.A. Davies, P.A. van der Merwe, Low affinity interaction of human or rat T cell adhesion molecule CD2 with its ligand aligns adhering membranes to achieve high physiological affinity, *J. Biol. Chem.* 272 (1997) 30889–30898.
- [10] K. Subramanian, C.J. Fee, R. Fredericks, R.S. Stubbs, M.T. Hayes, Insulin receptor–insulin interaction kinetics using multiplex surface plasmon resonance, *J. Mol. Recognit.* 26 (2013) 643–652.
- [11] C. Cruz, S.D. Santos, E.J. Cabrita, J.A. Queiroz, Binding analysis between L-histidine immobilized and oligonucleotides by SPR and NMR, *Int. J. Biol. Macromol.* 56 (2013) 175–180.
- [12] S. Ohlson, Designing transient binding drugs: a new concept for drug discovery, *Drug Discov. Today* 13 (2008) 433–439.
- [13] M.A. Cooper, Label-free screening of bio-molecular interactions, *Anal. Bioanal. Chem.* 377 (2003) 834–842.
- [14] S. Ray, G. Mehta, S. Srivastava, Label-free detection techniques for protein microarrays: prospects, merits and challenges, *Proteomics* 10 (2010) 731–748.
- [15] M.A. Cooper, V.T. Singleton, A survey of the 2001 to 2005 quartz crystal microbalance biosensor literature: applications of acoustic physics to the analysis of biomolecular interactions, *J. Mol. Recognit.* 20 (2007) 154–184.
- [16] P.G. Plagemann, Peptide ELISA for measuring antibodies to N-protein of porcine reproductive and respiratory syndrome virus, *J. Virol. Methods* 134 (2006) 99–118.
- [17] L. Liu, Y.-Y. Chen, Y.-H. Meng, S. Chen, G. Jin, Improvement for sensitivity of biosensor with total internal reflection imaging ellipsometry (TIRIE), *Thin Solid Films* 519 (2011) 2758–2762.
- [18] Y. Zhang, Y. Chen, G. Jin, Serum tumor marker detection on PEGylated lipid membrane using biosensor based on total internal reflection imaging ellipsometry, *Sensor. Actuat. B. Chem.* 159 (2011) 121–125.
- [19] L. Liu, A. Viallat, G. Jin, Vesicle adhesion visualized with total internal reflection imaging ellipsometry biosensor, *Sensor. Actuat. B. Chem.* 190 (2014) 221–226.
- [20] T. Kang, Y. Niu, G. Jin, Visualization of the interaction between tris and lysozyme with a biosensor based on total internal reflection imaging ellipsometry, *Thin Solid Films* 571 (2014) 463–467.
- [21] N. Bouropoulos, J. Moradian-Oldak, Analysis of hydroxyapatite surface coverage by amelogenin nanospheres following the Langmuir model for protein adsorption, *Calcif. Tissue Int.* 72 (2003) 599–603.
- [22] Y.B. Yang, C.N. Lim, J. Goodfellow, V.N. Sharifi, J. Swithenbank, A diffusion model for particle mixing in a packed bed of burning solids, *Fuel* 84 (2005) 213–225.
- [23] S.-C. Tsai, T.-H. Wang, Y.-Y. Wei, W.-C. Yeh, Y.-L. Jan, S.-P. Teng, Kinetics of Cs adsorption/desorption on granite by a pseudo first order reaction model, *J. Radioanal. Nucl. Chem.* 275 (2007) 555–562.
- [24] G. Jin, Y.H. Meng, L. Liu, Y. Niu, S. Chen, Q. Cai, T.J. Jiang, Development of biosensor based on imaging ellipsometry and biomedical applications, *Thin Solid Films* 519 (2011) 2750–2757.
- [25] W. Rudzinski, W. Plazinski, Studies of the kinetics of solute adsorption at solid/solution interfaces: on the possibility of distinguishing between the diffusional and the surface reaction kinetic models by studying the pseudo-first-order kinetics, *J. Phys. Chem. C* 111 (2007) 15100–15110.
- [26] R.M.A. Azzam, N.M. Bashara, *Ellipsometry and Polarized Light*, first ed., 1987. North Holland.
- [27] M. Born, E. Wolf, *Principles of Optics*, first ed., Cambridge University Press, 1999.
- [28] L. Quan, D. Wei, X. Jiang, Y. Liu, Z. Li, N. Li, K. Li, F. Liu, L. Lai, Resurveying the Tris buffer solution: the specific interaction between tris(hydroxymethyl)aminomethane and lysozyme, *Anal. Biochem.* 378 (2008) 144–150.
- [29] P. Nelson, *Biophysics*, second ed., Shanghai Scientific and Technical Publishers, 2006.